Electronic Supplementary Material (ESI) for Journal of Materials Chemistry A.

Supporting Information

A diamine-grafted metal-organic framework with top-performing CO_2 capture properties and a facile coating approach for imparting exceptional moisture stability

Minjung Kang,‡[a] Jeong Eun Kim,‡[a] Dong Won Kang,[a] Hwa Young Lee,[a] Dohyun Moon,[b] and Chang Seop Hong[a]*

[a]*Department of Chemistry, Korea University, Seoul 136-713, Republic of Korea.*

[b]*Beamline Division, Pohang Accelerator Laboratory, Pohang, Kyungbuk 790-784, Republic of Korea.*
**Email - cshong@korea.ac.kr ‡ Joint contributors*

Preparation.

All chemicals and solvents in the synthesis were reagent grade and used as received. H_4dobpdc was prepared according to the literature.[1]

[M_2(dobpdc)(een)$_x$(H_2O)$_y$] [een-M_2(dobpdc)]. We used the same procedure with the synthesis of **1-een**. Elemental analysis (%) calcd for [Mg_2(dobpdc)(een)$_{1.7}$(H_2O)$_{0.3}$] (H_2O)$_{1.5}$ (een-Mg_2(dobpdc)·1.1H_2O): C 49.86, H 6.03, N 9.50; found: C 49.62, H 5.74, N 9.23. [Co_2(dobpdc)(een)$_{1.85}$(H_2O)$_{0.15}$](H_2O)$_{1.55}$ (een-Co_2(dobpdc)·1.55H_2O): C 44.18, H 5.47 , N 8.91; found: C 44.19, H 5.11, N 9.01. [Ni_2(dobpdc)(een)$_{1.9}$(H_2O)$_{0.1}$](H_2O)$_{1.1}$ (een-Ni_2(dobpdc)·1.1H_2O): C 44.99, H 5.45 , N 9.23; found: C 44.69, H 5.4, N 9.56. [Zn_2(dobpdc)(een)$_{1.9}$(H_2O)$_{0.1}$](H_2O)$_{1.5}$ (een-Zn_2(dobpdc)·1.5H_2O): C 43.60, H 5.52, N 9.24; found: C 43.92, H 5.62, N 9.15. To check the structural change upon CO_2 adsorption, we exposed een-M_2(dobpdc) to 100% CO_2 at 40 °C for 30 min, affording een-M_2(dobpdc)-CO_2. een-M_2(dobpdc)-regenerated was obtained by heating een-M_2(dobpdc)-CO_2 at 140 °C (Mg) and 120 °C (Co, Ni, Zn) for 30 min. Synchrotron PXRD data were collected to analyse the cell volume variation during CO_2 adsorption and regeneration (Fig. S1).

Powder X-ray Diffraction and Structure Modeling. PXRD data were recorded using Cu Kα (λ = 1.5406 Å) on a Rigaku Ultima III diffractometer with a scan speed of 2°/min and a step size of 0.01°. The synchrotron powder X-ray diffraction data were collected at 298 K with the 240 mm of detector distance in 2400 s exposure with synchrotron radiation (λ = 1.09998 Å) using a 2D SMC ADSC Quantum-210 detector with a silicon (111) double crystal monochromator at the Pohang Accelerator Laboratory. The ADX program[2] was used for data collection, and Fit2D program[3] was used for converting a two-dimensional diffraction image to a one-dimensional diffraction pattern. The unit cell dimensions of **1-een, 1-een-CO_2, and 1-een-regenerated** were determined by conducting a full-pattern decomposition with the Le Bail method (Pawley refinement) implemented in *TOPAS-Academic*. The trigonal space group $P3_221$ was utilized for the refinements, due to the isomorphism with Zn_2(dobpdc).[1] Based on the unit cell dimensions obtained, the geometry of the backbones was optimized via an energy minimization algorithm using the universal force field implemented in the *Forcite* module of *Materials Studio*.[4]

Gas Sorption Measurements. Gas sorption isotherms were measured using a Micromeritics 3FLEX instrument up to 1 atm of gas pressure unless otherwise stated. The highly pure N_2 (99.999%) and CO_2 (99.999%) were used in the sorption experiments. N_2 gas isotherms were measured at 77 K and CO_2 uptake was measured at 298 K, 313 K, 333 K, 353 K, 373K, 393 K, 403 K, 413 K, and 423 K.

Thermogravimetric Analyses and Gas Cycling Measurements. Thermogravimetric analyses (TGA) were carried out at a ramp rate of 2 °C/min in an Ar (99.999 %) flow using a Scinco TGA N-1000 instrument and TA instrument Discovery TGA. CO_2 cycling experiments of the activated **1-een** were carried out on the instrument with 15% CO_2 in N_2. A flow rate of 70 mL/min was applied for all gases.

Infrared Spectroscopy Measurements. In situ IR spectra were obtained with an air-tight homemade IR cell composed of KBr windows by using a Nicolet iS10 FTIR spectrometer. Before the IR measurements, high-purity N_2 (99.999%) was purged into the sample chamber, detector, and IR source to remove atmospheric CO_2 from the IR spectrometer. We also recorded IR spectra with an attenuated total reflectance (ATR) module by using Nicolet iS10 FTIR spectrometer.

Other Physical Measurement. Adsorption properties in the wet streams were measured by an automated chemisorption analyzer (Micromeritics Autochem II 2920). Elemental analyses for C, H, and N were performed at the Elemental Analysis Service Center of Sogang University. XPS was measured at Semiconductor & Display Green Manufacturing Research Center (GMRC) at Korea University. Contact angle was measured by Phoenix-MT(T). SEM images were measured by S-4600 at Korea Basic Science Institute (KBSI). TEM analyses were measured by XFEG-Titan 300 kV FE-TEM by S-4600 at Korea Basic Science Institute (KBSI).

[Reference]

1. T. M. McDonald, W. R. Lee, J. A. Mason, B. M. Wiers, C. S. Hong and J. R. Long, *J. Am. Chem. Soc.*, 2012, **134**, 7056-7065.

2. A. J. Arvai, C. Nielsen, ADSC Quantum-210 ADX Program, Area Detector System Corporation; Poway, CA, USA, 1983.

3. Fit2D Program: Hammersley, A. (E-mail: hammersley@esrf.fr), ESRF, 6 RUE JULES HOROWITZ BP 220 38043 GRENOBLE CEDEX 9 FRANCE.

4. H. Deng, S. Grunder, K. E. Dordova, C. Valente, H. Furukawa, M. Hmadeh, F. Gándara, A. C. Whalley, Z. Liu, S. Asahina, H. Kazumori, M. O'Keeffe, O. Terasaki, J. F. Stoddart, O. M. Yaghi, *Science* 2012, **336**, 1018-1023.

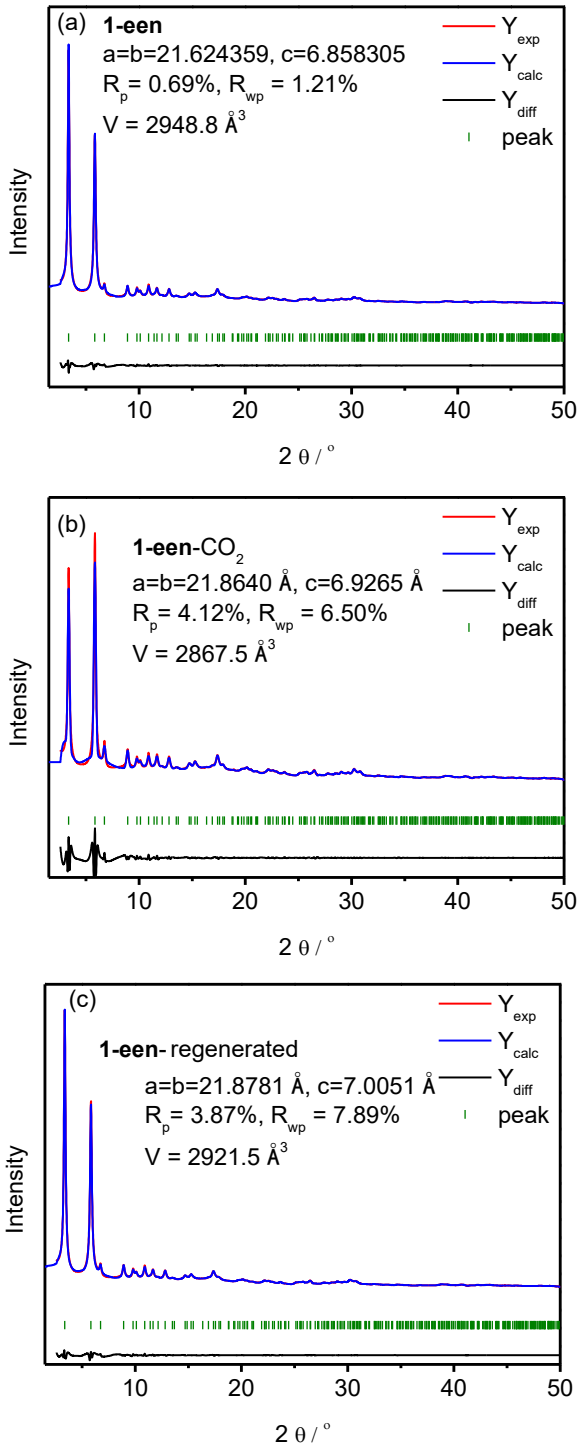

Fig. S1. Synchrotron powder X-ray diffraction pattern of (a) **1-een**, (b) **1-een**-CO_2, and (c) **1-een**-regenerated (red) with calculated diffraction patterns (blue) from Pawley refinement. The difference is shown in black.

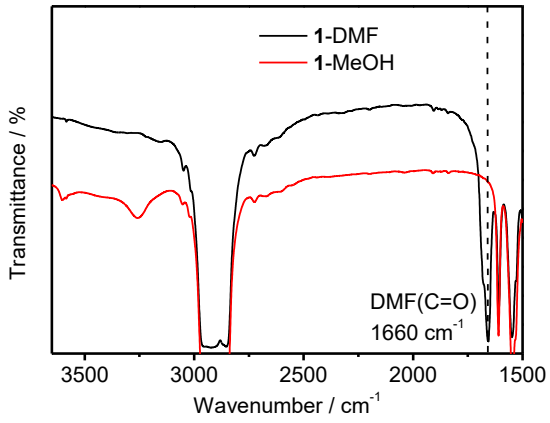

Fig. S2. FT-IR data of **1**-DMF and **1**-MeOH.

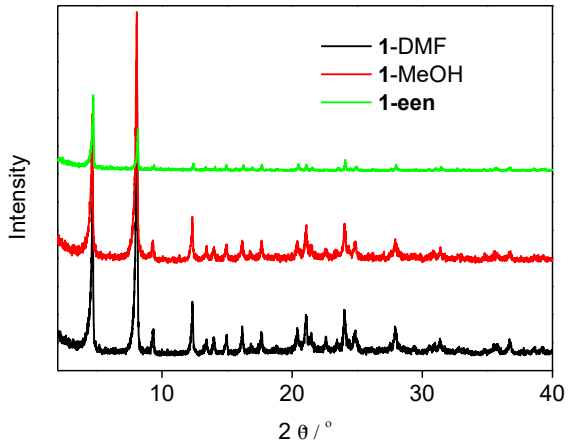

Fig. S3. Powder X-ray diffraction pattern of **1**-DMF, **1**-MeOH, and **1-een**.

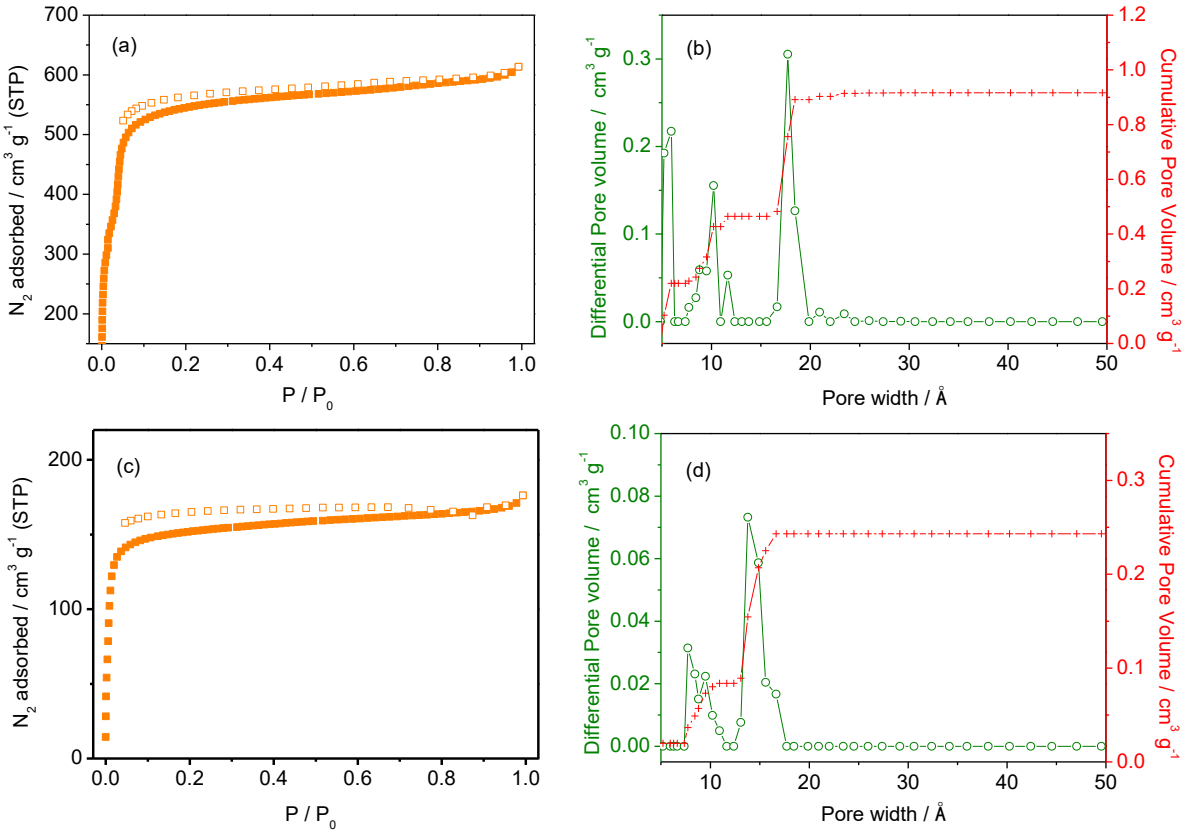

Fig. S4. N_2 adsorption isotherms of (a) **1** and (c) **1-een** at 77 K.. DFT pore size distribution for (b) **1** and (d) **1-een** calculated from N_2 adsorption at 77 K using a Tarazona NLDFT with a cylinder pore geometry.

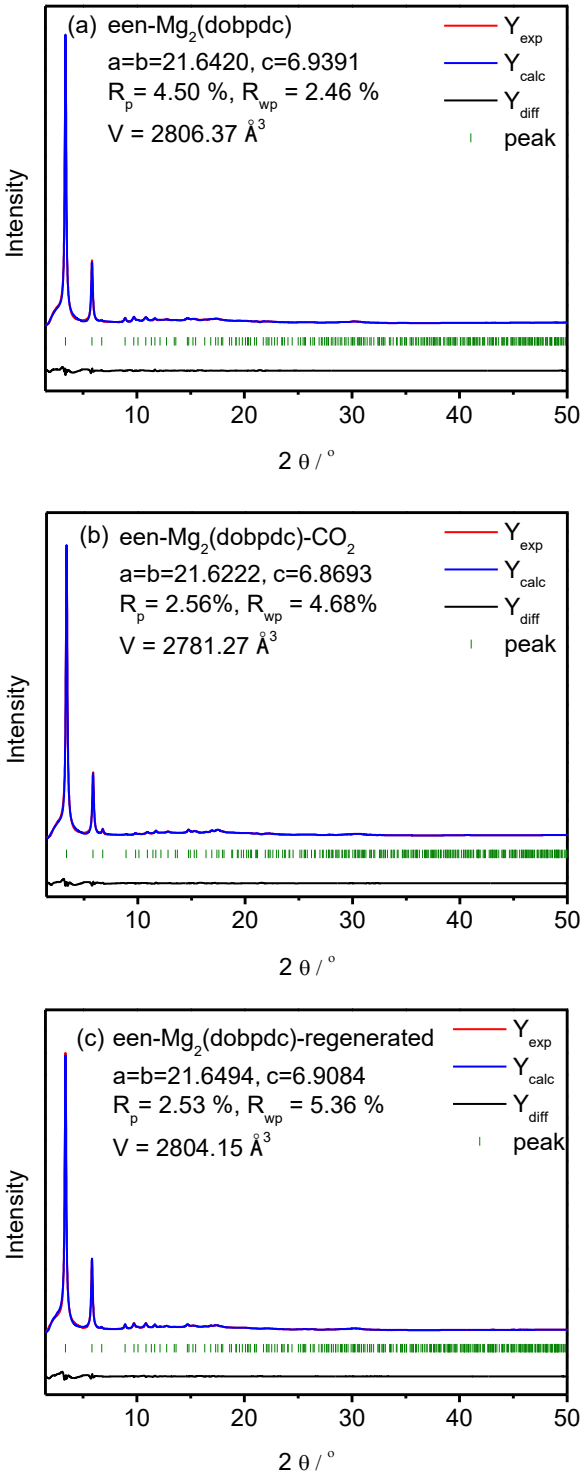

Fig. S5. Synchrotron powder X-ray diffraction pattern of (a) een-Mg_2(dobpdc), (b) een-Mg_2(dobpdc)-CO_2, and (c) een-Mg_2(dobpdc)-regenerated (red) with calculated diffraction patterns (blue) from Pawley refinement. The difference is shown in black.

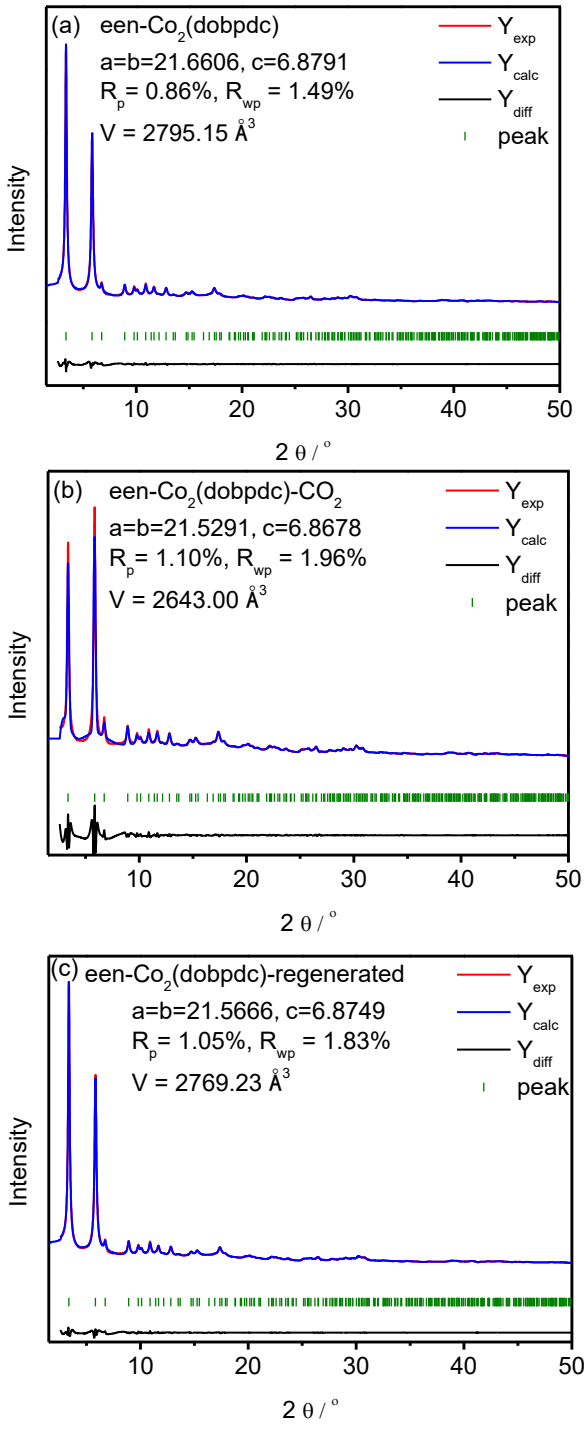

Fig. S6. Synchrotron powder X-ray diffraction pattern of (a) een-Co_2(dobpdc), (b) een-Co_2(dobpdc)-CO_2, and (c) een-Co_2(dobpdc)-regenerated (red) with calculated diffraction patterns (blue) from Pawley refinement. The difference is shown in black.

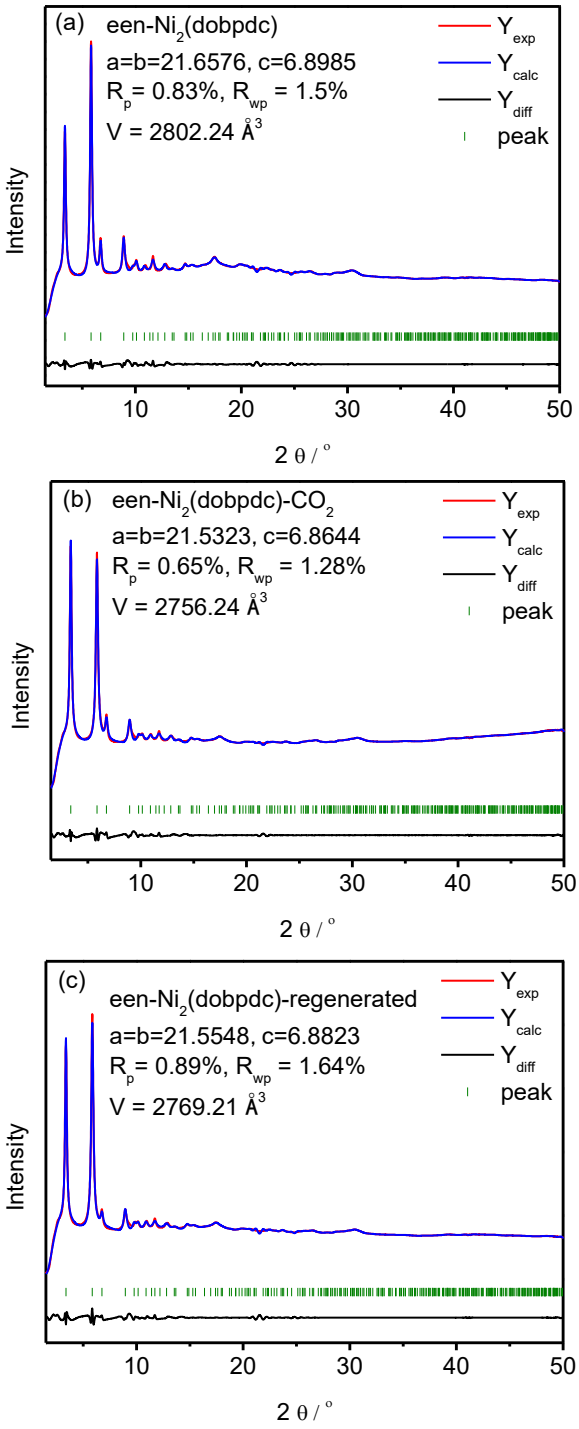

Fig. S7. Synchrotron powder X-ray diffraction pattern of (a) een-Ni_2(dobpdc), (b) een-Ni_2(dobpdc)-CO_2, and (c) een-Ni_2(dobpdc)-regenerated (red) with calculated diffraction patterns (blue) from Pawley refinement. The difference is shown in black.

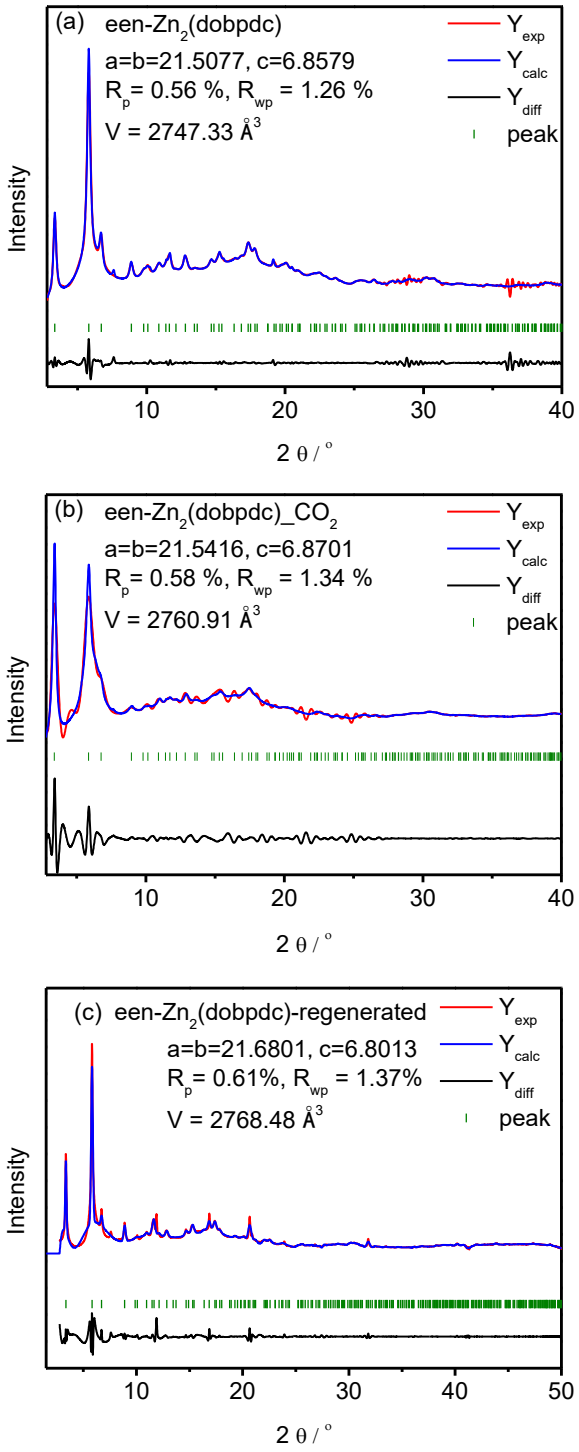

Fig. S8. Synchrotron powder X-ray diffraction pattern of (a) een-Zn_2(dobpdc), (b) een-Zn_2(dobpdc)-CO_2, and (c) een-Zn_2(dobpdc)-regenerated (red) with calculated diffraction patterns (blue) from Pawley refinement. The difference is shown in black.

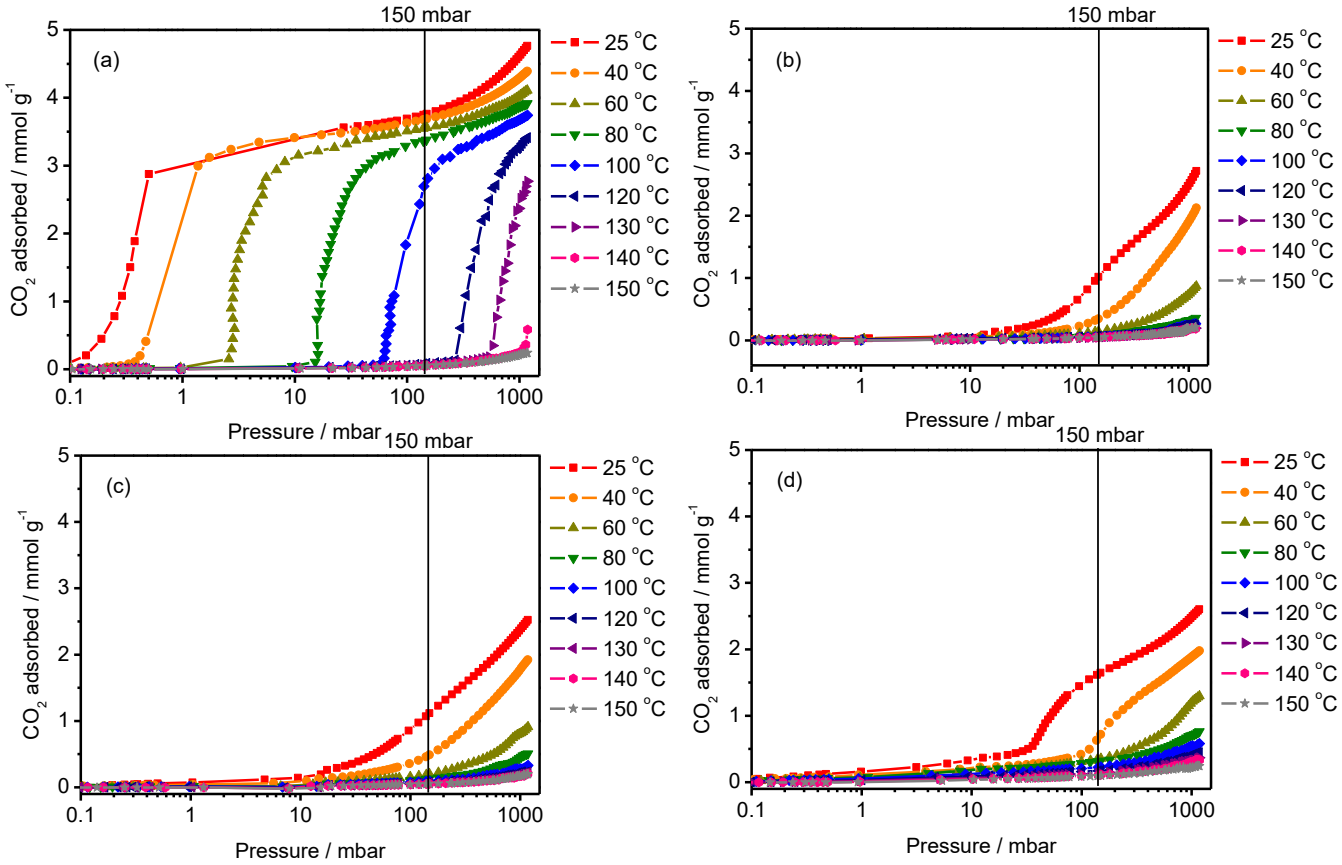

Fig. S9. Adsorption isotherms of CO_2 for een-M_2(dobpdc) with M = (a) Mg, (b) Co, (c) Ni, and (d) Zn at the indicated temperatures. The CO_2 partial pressure of flue gas (150 mbar CO_2) is highlighted by dashed lines. The solid lines are eye-guides.

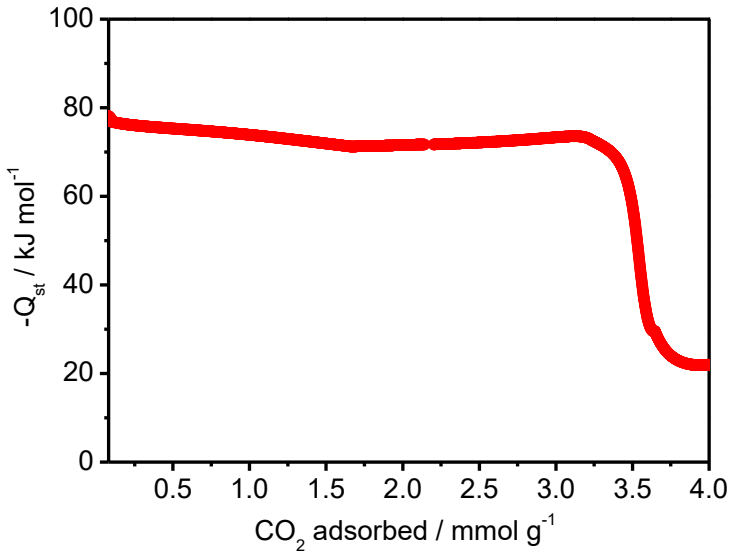

Fig. S10. Isosteric heat of CO_2 adsorption onto **1-een**.

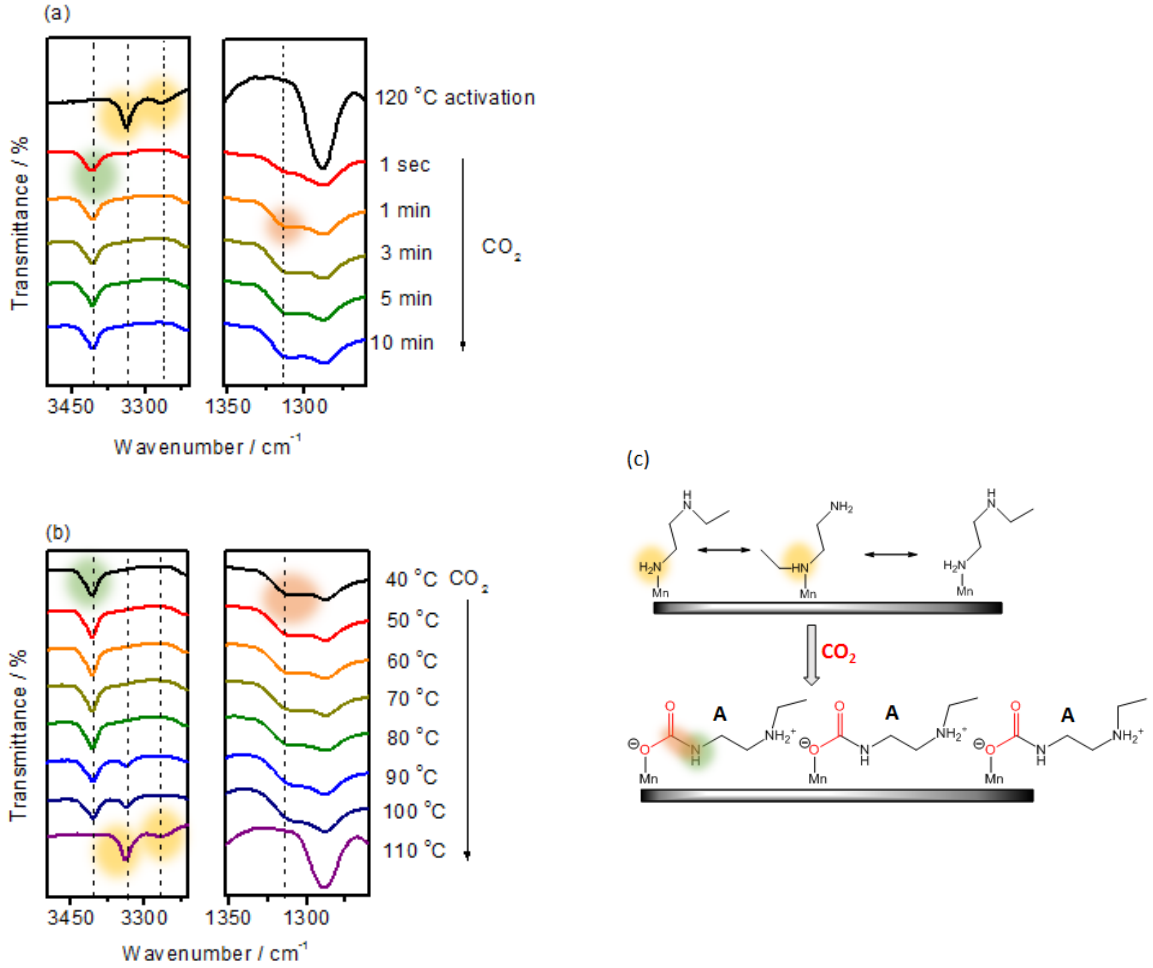

Fig. S11. (a) In situ IR spectra of **1-een** in the high- and low-frequency regions showing N-H stretching and C-N vibration, respectively. The IR data represent the peak variations over time under a flow of 100% CO_2. (b) In situ IR spectra of **1-een** under a 100% CO_2 stream with increasing temperature. (c) One of possible CO_2 adsorption mechanism with AA mode showing CO_2 insertion between Mn-N(primary) in carbamate unit. If CO_2 inserted into between Mn-N(secondary), it is assigened as B mode. Therefore, there are four possible modes of AA, AB, BA, and BB. The color indicates the vibrations of functional groups corresponding to the IR peaks in (a) and (b). The free amines could be subject to hydrogen binding between neighboring amine groups.

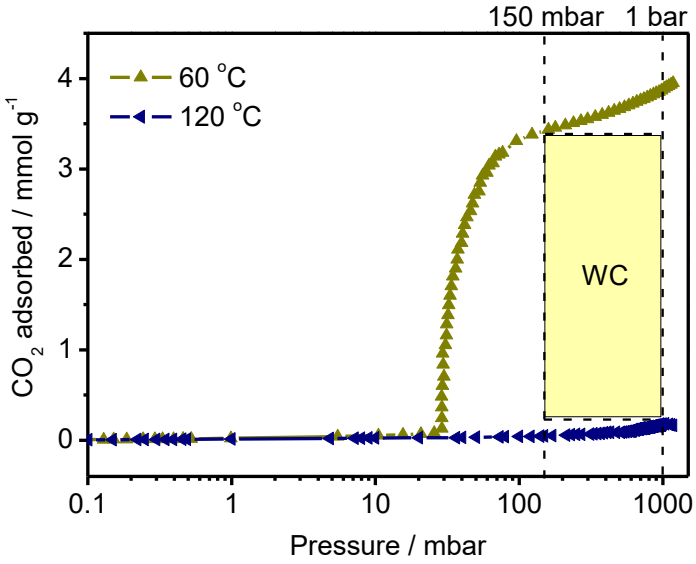

(a)

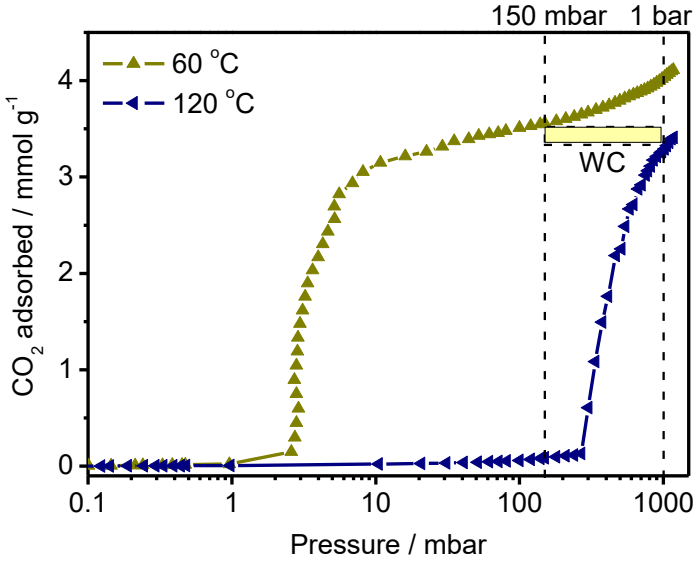

(b)

Fig. S12. Working capacities (WC) for (a) **1-een** and (b) een-Mg_2(dobpdc) calculated by the difference between adsorbed amount at 60 ºC and 15% CO_2, and that at 120 ºC and 100% CO_2.

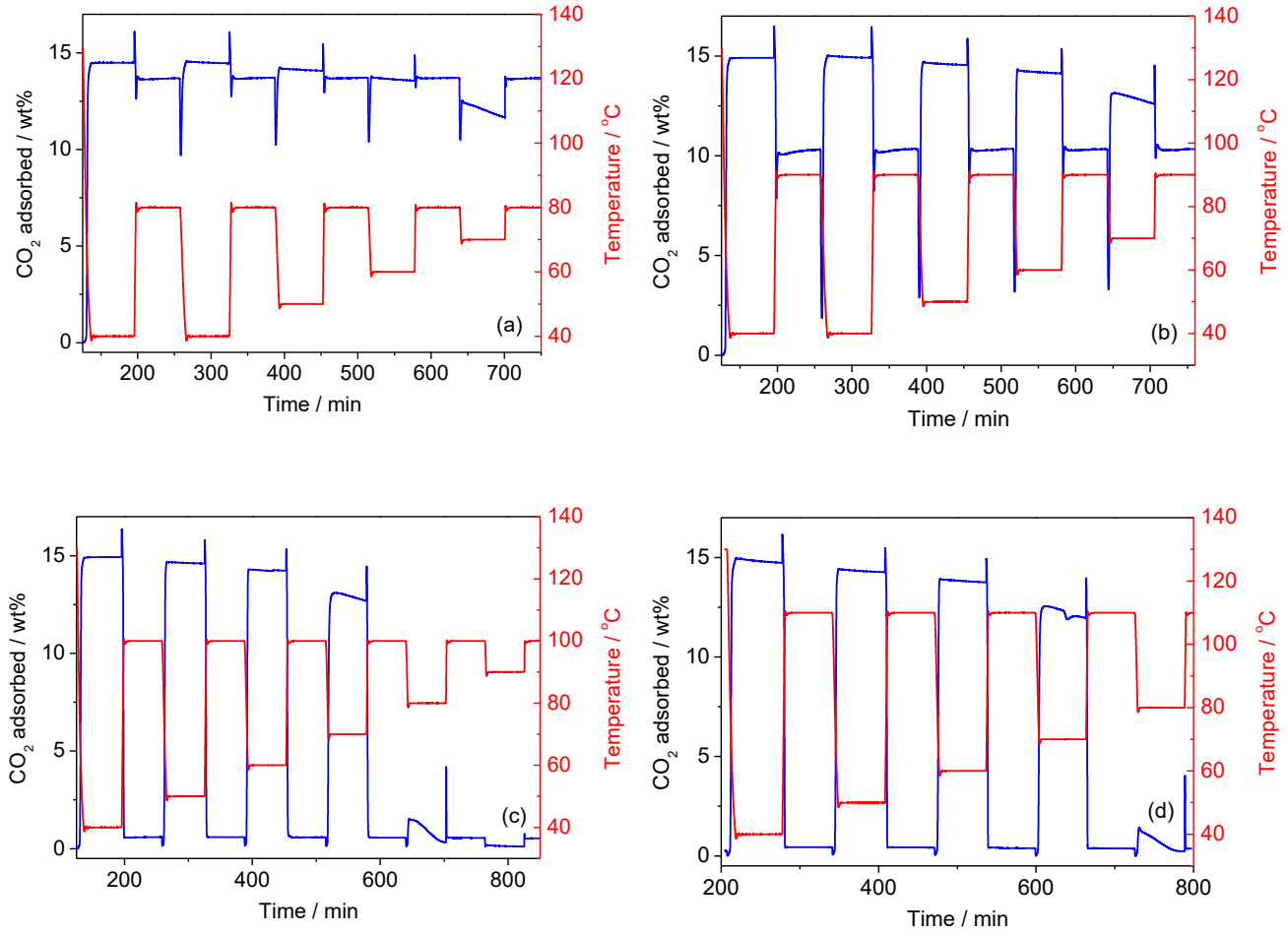

Fig. S13. TGA curves (blue lines) for **1-een**, at desorption temperature (T_{des}) of (a) 80 ºC, (b) 90 ºC, (c) 100 ºC, and (d) 110 ºC. The temperature profiles are represented by red lines. Adsorption occurred at increased temperatures and 15% CO_2 for 60 min and desorption occurred at different temperatures (T_{des}) and under pure CO_2 flowing for 60 min.

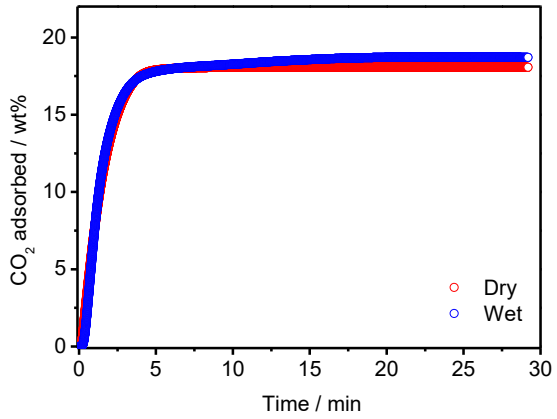

Fig. S14. Adsorption capacity of **1-een** under dry (15% CO_2 and 85% He) and wet (15% CO_2, 3.75% H_2O, and 81.25% He) conditions. The flow rate of the mixed gas was 80 mL/min.

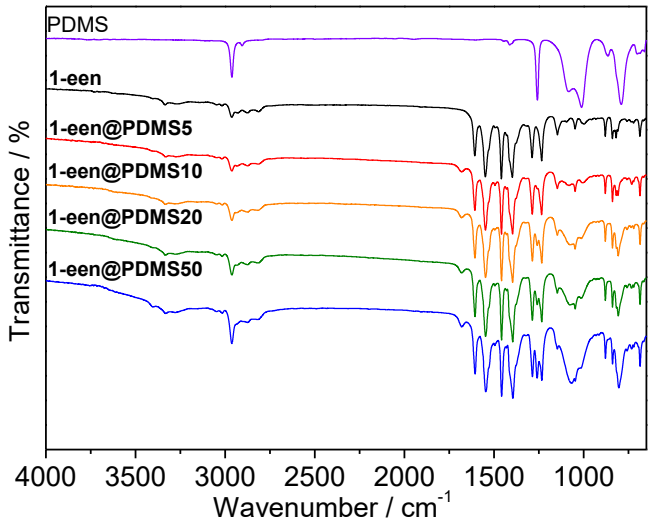

Fig. S15. IR spectra of PDMS, **1-een**, and PDMS-coated samples.

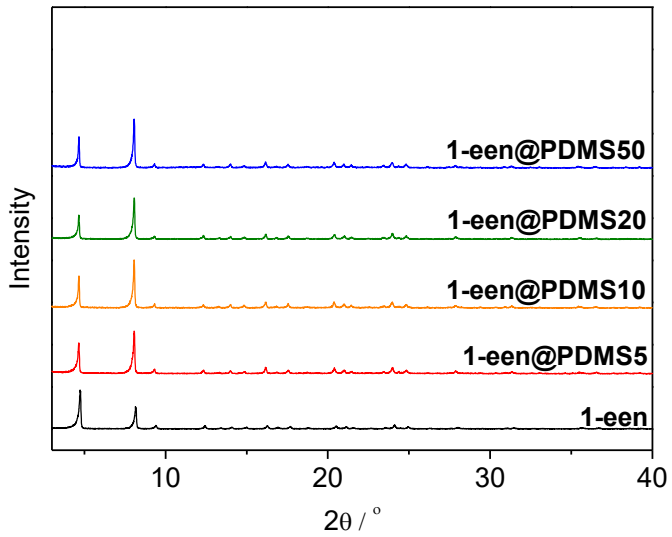

Fig. S16. PXRD profiles of **1-een** coated by PDMS with different loading concentrations.

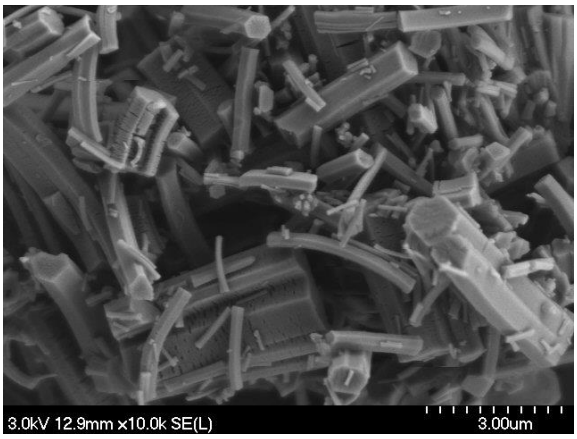

(a)

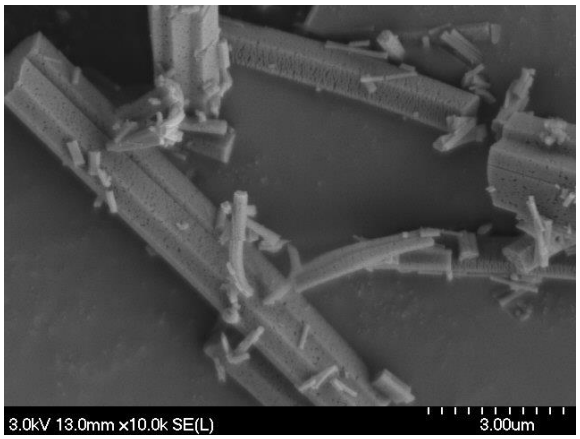

(b)

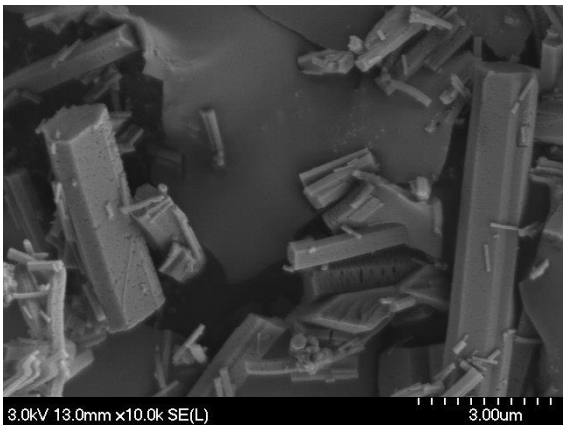

(c)

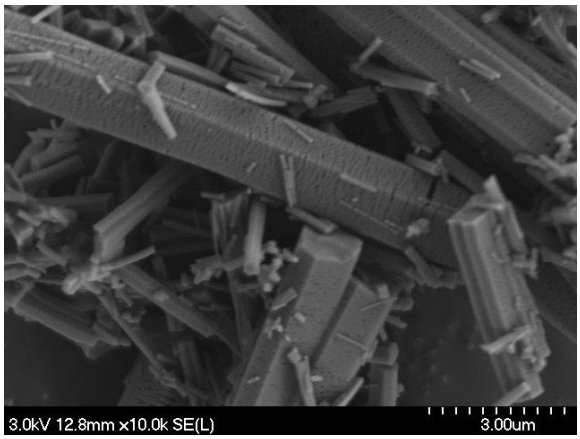

(d)

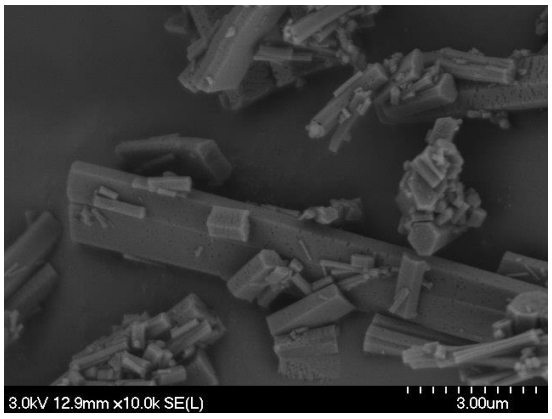

(e)

Fig. S17. SEM images of (a) **1-een**, (b) **1-een@PDMS5**, (c) **1-een@PDMS10**, (c) **1-een@PDMS20**, and (d) **1-een@PDMS50**.

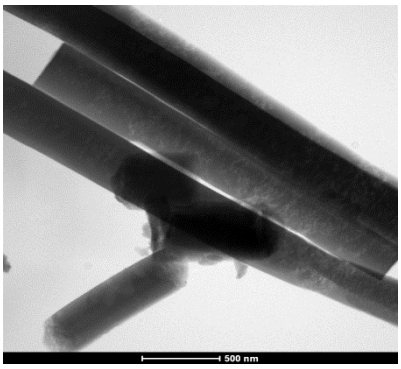

(a)

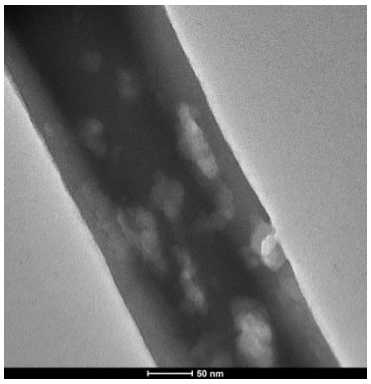

(b)

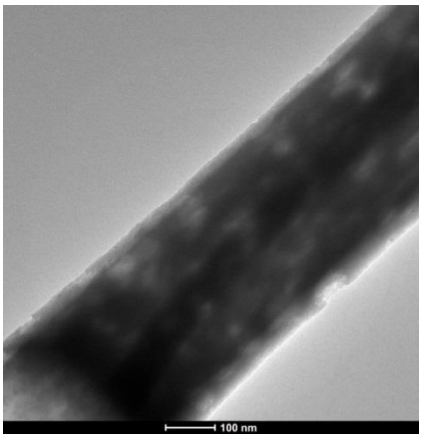

(c)

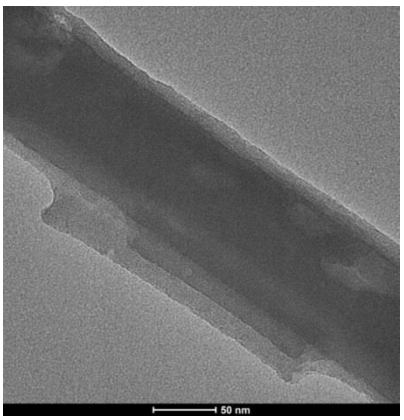

(d)

Fig. S18. High resolution TEM images of (a) **1-een**, (b) **1-een@PDMS5**, (c) **1-een@PDMS10**, and (d) **1-een@PDMS50**.

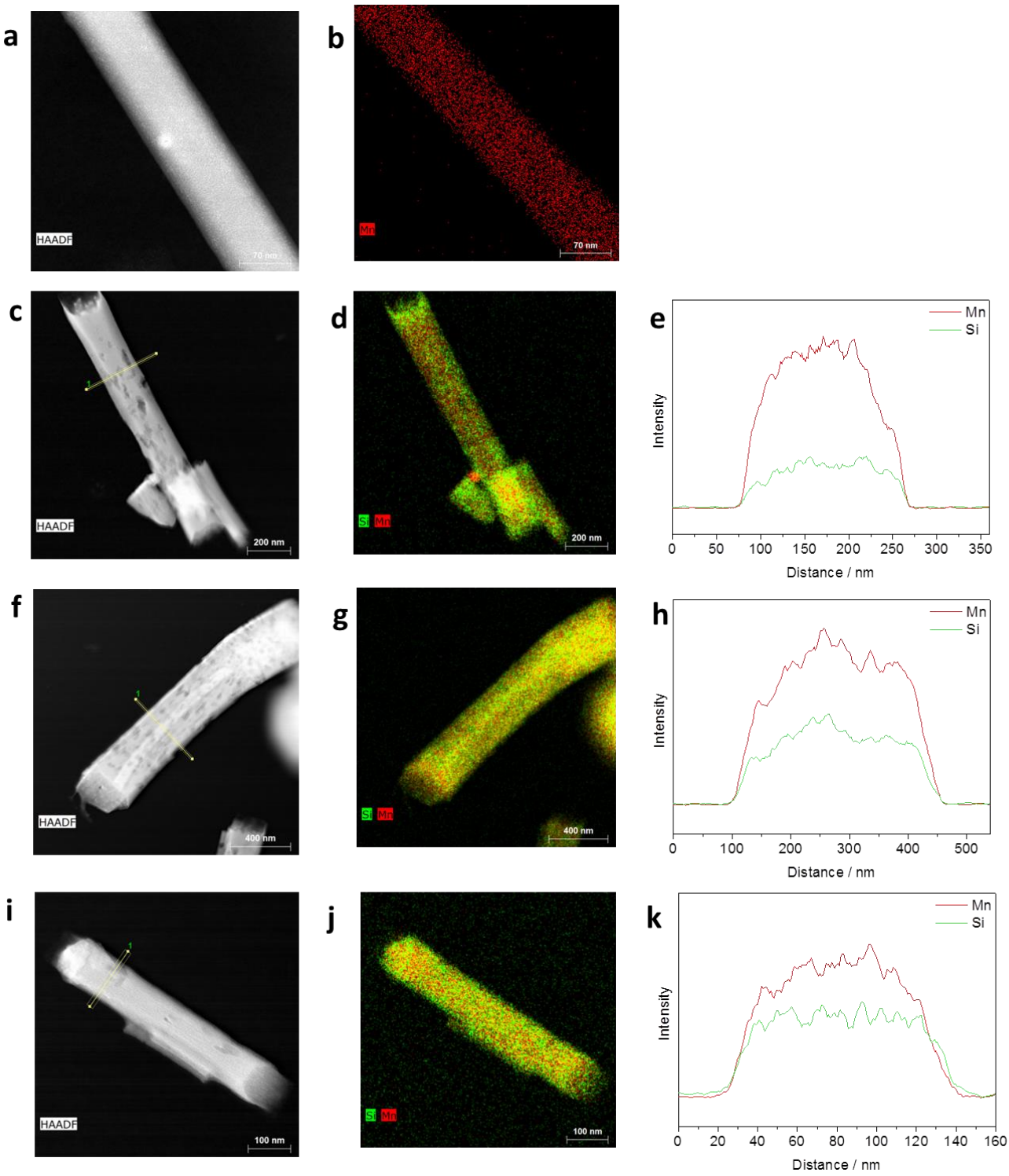

Fig. S19. STEM images of (a) **1-een**, (c) **1-een@PDMS5**, (f) **1-een@PDMS10**, and (i) **1-een@PDMS50**. Elemental mapping analysis of (b) **1-een**, (d) **1-een@PDMS5**, (g) **1-een@PDMS10**, and (j) **1-een@PDMS50**. Cross-sectional line profiles of data of (e) **1-een@PDMS5**, (h) **1-een@PDMS10**, and (k) **1-een@PDMS50**.

Table S1. Compositional analysis (atomic%) of Mn and Si determined by the line-scan profiles.

1-een@PDMS5		**1-een@PDMS10**		**1-een@PDMS20**		**1-een@PDMS50**	
Mn(%)	Si(%)	Mn(%)	Si(%)	Mn(%)	Si (%)	Mn (%)	Si (%)
74.15	25.85	65.55	34.45	62.68	37.32	58.64	41.36

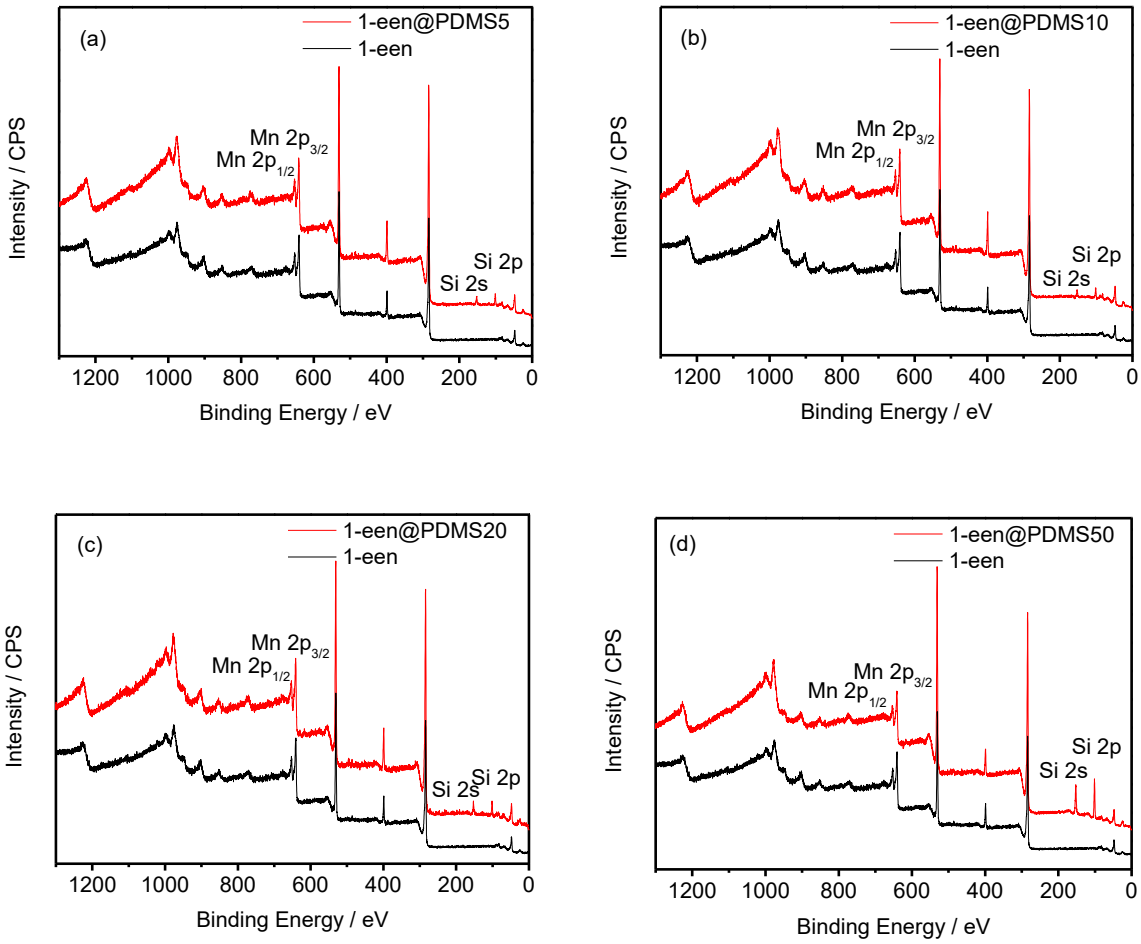

Fig. S20. XPS of (a) **1-een@PDMS5**, (b) **1-een@PDMS10**, (c) **1-een@PDMS20**, and (d) **1-een@PDMS50** with the reference of **1-een**.

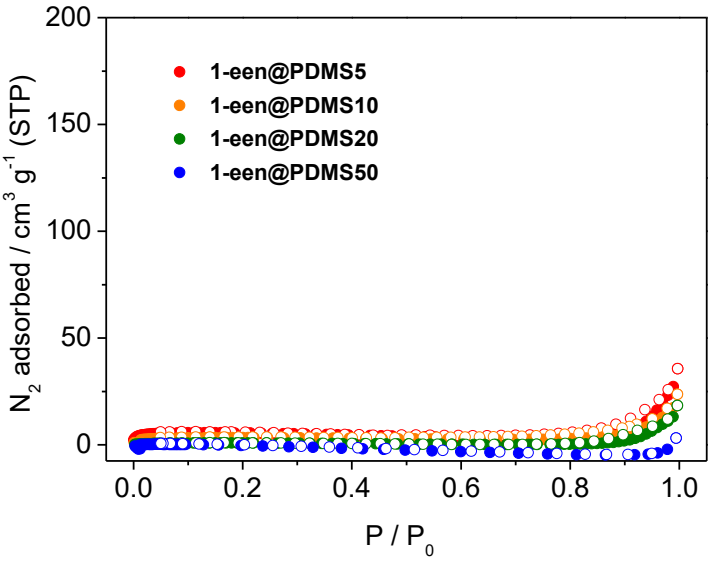

Fig. S21. N_2 isotherms of the coated samples at 77 K.

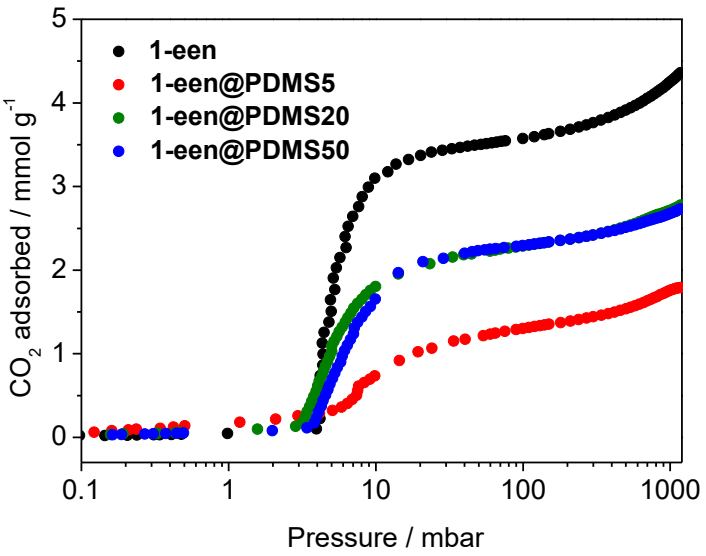

Fig. S22. CO_2 isotherms of **1-een** and the coated samples at 313 K.

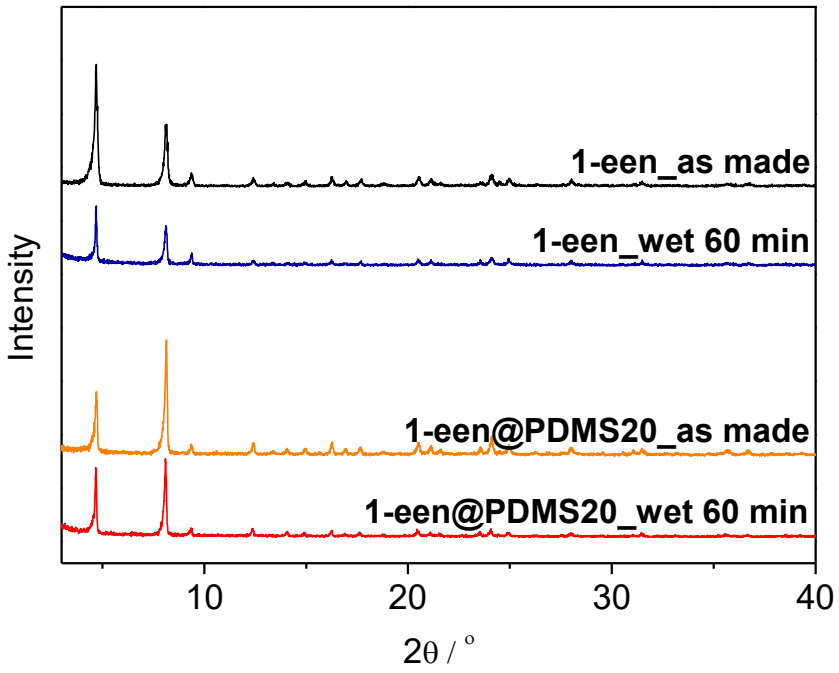

Fig. S23. PXRD profiles of **1-een** and **1-een@PDMS20** before and after exposure to 100% relative humidity at room temperature.

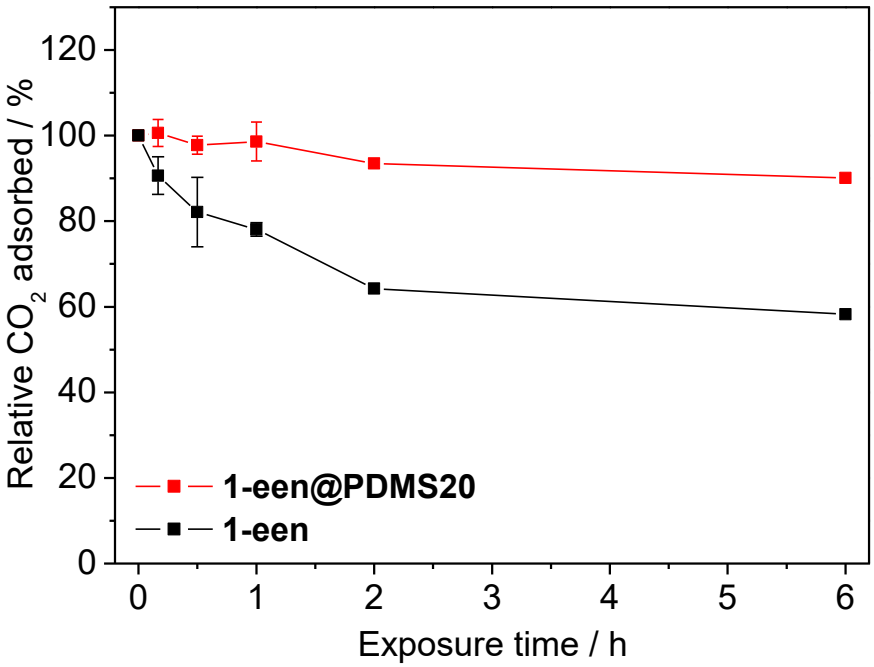

Fig. S24. Relative CO_2 uptake of **1-een** and **1-een@PDMS20** before and after exposure to water vapor up to 6 h.

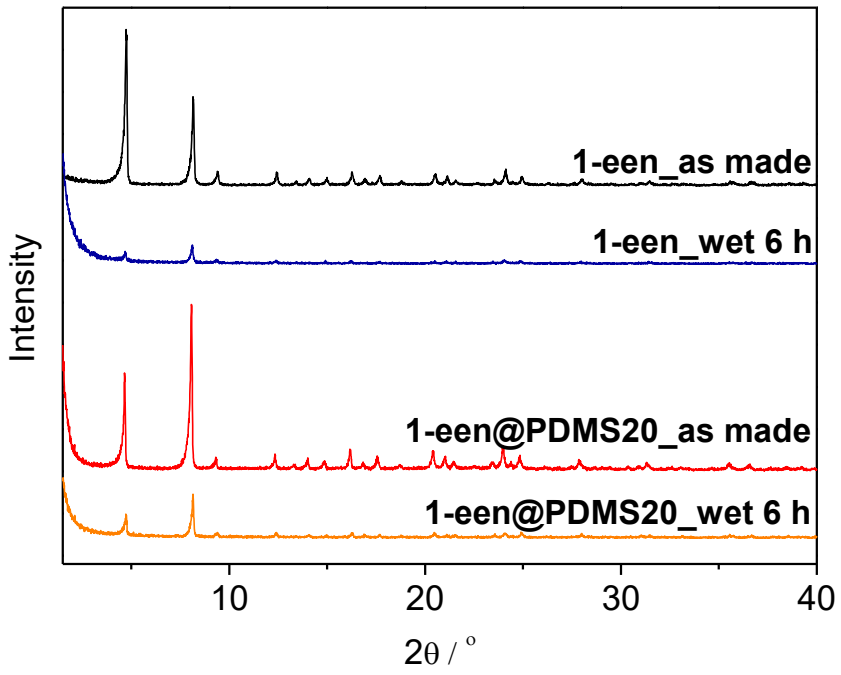

Fig. S25. PXRD profiles of **1-een** and **1-een@PDMS20** before and after exposure to 100% relative humidity at room temperature.

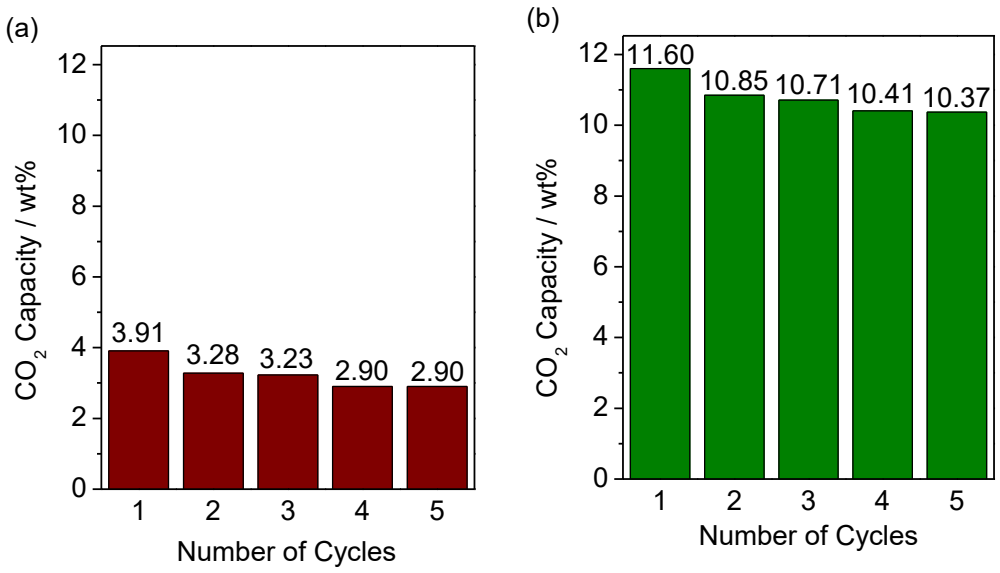

Fig. S26. Cyclic CO_2 adsorption capacity for (a) **1-een** and (b**) 1-een@PDMS20** under wet streams (15% CO_2, 3.75% H_2O, and 81.25% He), measured by Autochem II 2920. Adsortion occurred at 70 ºC for 30 min and desorption occurred at 100 ºC for 30 min.